Hindawi
Advances in Civil Engineering
Volume 2019, Article ID 8438639, 13 pages
https://doi.org/10.1155/2019/8438639

Research Article

Multiobjective Optimization Design for Structural Parameters of TBM Disc Cutter Rings Based on FAHP and SAMPGA

Laikuang Lin,[1,2] **Yimin Xia**,[1,2] **and Dun Wu**[3]

[1]*College of Mechanical and Electrical Engineering, Central South University, Changsha 410083, China*
[2]*State Key Laboratory of High Performance Complex Manufacturing, Central South University, Changsha 410083, China*
[3]*China Railway 14th Bureau Group Tunnel Engineering Co., Ltd., Jinan 250014, China*

Correspondence should be addressed to Laikuang Lin; linlaikuang@csu.edu.cn and Yimin Xia; xiaymj@csu.edu.cn

Received 11 July 2019; Accepted 22 August 2019; Published 12 September 2019

Guest Editor: Moacir Kripka

As a key component of tunnel boring machines (TBMs), the disc cutter ring and its structural parameters are closely related to the TBM tunneling quality. Literature review shows that investigations on optimization design methods for cutter ring structure are seriously insufficient. Therefore, in this paper, a multiobjective optimization design model of structural parameters for disc cutter rings is developed based on the complex geological conditions and the corresponding cutter ring structure design requirements. The rock breaking capability, energy consumption, load-bearing capability, wear life, and wear uniformity of disc cutter are selected as the objectives, and the geometric structure of cutter rings, ultimate load-bearing capability, and cutterhead drive performance are determined as constraints. According to the characteristics of this model, a self-adaptive multipopulation genetic algorithm (SAMPGA) is utilized to solve the optimization problem, and the Fuzzy analytical hierarchy process (FAHP) is employed to calculate weight coefficients for multiple objectives. Finally, the applicability of the proposed method is demonstrated through a case study in a TBM project. The results indicated that the rock breaking performance and service life of the disc cutter are improved after optimization by using the proposed method. The utilization of SAMPGA effectively solves the premature local convergence problems during optimization. The geological adaptability should be considered in the cutter ring structure design, which can be realized by using the proposed method based on the suitable weight coefficients.

1. Introduction

With the rapid development of tunnel constructions, tunnel boring machines (TBMs) are widely employed in tunnel excavation due to their high excavation efficiency, excellent safety, and less ground disturbance [1, 2]. Disc cutters mounted on TBM cutterhead are the main rock breaking tools, and cutter rings interact with and cut rocks directly during the TBM tunneling process [3, 4]. When tunneling in the complex and harsh geological conditions, the cutter ring suffers from high contact stress and strong impact vibration. If the structural design of the cutter ring is unreasonable, it will not only limit the rock breaking capability and efficiency of the disc cutter but also cause serious wear and breakage failure of the cutter ring, which will significantly affect the tunneling efficiency and construction cost of the TBM project. Nowadays, most of the existing cutter ring designs are based on engineering experience or adopt commonly used dimensions specified by several well-known cutter manufacturers. Relevant optimization design method for structural parameters of TBM disc cutter ring is rare. Therefore, it is of great necessity and attractiveness to develop geological adaptability and a multiobjective optimization design method for cutter ring structural parameters on the basis of the complex and changeable geological conditions.

At present, the research associated with cutter ring structure mainly focuses on the rock breaking characteristics of types of cutter rings and the influence of cutter ring structural parameters on its cutting performance. Rostami [5] studied the load characteristics and rock fragmentation induced by a disc cutter based on linear cutting experiments

and pointed out that the contact stress of cutter ring is closely related to the cutter tip width. Balci and Tumac [6, 7] compared and analyzed the rock breaking loads of constant cross-section (CCS) and V-type disc cutters through a series of rock breaking tests, and they established and modified the rock breaking load prediction model of the CCS disc cutter considering the influences of diameter, tip width, and edge angle of cutter ring. Choi et al. [8] investigated the effects of cutter ring shape on cutter forces by a series of full-scale linear cutting tests and found that the rolling stress acting on a V-shape disc cutter was much higher than on a CCS disc cutter. Chiaia [9] studied the rock breaking mechanisms using different types of cutters, including blunt rigid sphere, flat punch, and circular cone. Lislerud [10] compared the rock breaking characteristics of flat-edged disc cutter, wedge-shaped disc cutter, and studded roller disc cutter and put forward the rock breaking kinetic model of studded roller disc cutter. Zhang et al. [11] studied the rock fragmentation process subject to wedge cutters by physical experiments and bonded particle model simulations, and the AE distribution, crack pattern, and cutter force were obtained both for single cutter and double cutters. Roby et al. [12] introduced recent improvements in the disc cutter components and emphatically analyzed the distinctions of disc cutters with different sizes. Maidl et al. [13] presented that the cutter tip widths of commonly used disc cutters are mainly designed as 6.35 mm (1/4-inch), 12.7 mm (1/2-inch), 19.05 mm (3/4-inch), and 25.4 mm (1-inch). Marji [14] and Sun et al. [15] established rock breaking simulation models for disc cutters by using discrete element method and revealed the effects of cutter tip width and edge angle parameters on the cutter rock breaking performance (crack propagation, rock breaking volume, specific energy, etc.). Li et al. [16] analyzed the difference in rock breaking characteristics between small edge angle cutter ring and fat edge cutter ring through theoretical, simulation, and experimental analysis, and they found the performance of the small edge angle cutter ring better than that of the fat edge cutter ring in high abrasive strata. Xia et al. [17] used the orthogonal test method to analyze the influences of cutter ring structural parameters on rock breaking forces. Review of the literature shows that researches on cutter ring structural design mainly focus on the effects of the shape size or structural parameters of the cutter ring on its rock breaking performance based on parametric analysis method. However, the effects of cutter ring structural parameters on other cutter performances, e.g., wear resistance performance, are seldom considered as well as the influence of geological conditions on the structural design of cutter rings. In reality, disc cutter wear is an important factor that raises up the excavation cost and delays the project during TBM tunneling of hard rock [18]. Additionally, investigations on multiobjective optimization design methods for cutter ring structural parameters are seriously insufficient.

Cutter ring structural design problem contains several mutually conflicting objectives and constraints, which belong to a multiobjective optimization problem. To deal with this engineering problem, selecting a suitable multiobjective optimization approach is one of the aims in this study. Traditional optimization techniques tend to provide a local optimum solution in scenarios where the size of the search space is large, a number of variables are to be handled, multiple objectives are to be achieved, and a number of constraints are to be satisfied simultaneously [19]. Therefore, a number of population-based optimization algorithms known as the advanced optimization algorithms have been developed in recent year and extensively used in engineering issues. These methods mainly include genetic algorithm (GA) [20], particle swarm optimization (PSO) [21], artificial immune system [22], differential evolution algorithms [23], ant colony algorithm (ACA) [24], and simulated annealing (SA) [25]. As a classical meta-heuristic algorithm, GA is frequently used as a search strategy to discover the optimal subset. However, there are some defects existed in simple GA (SGA), such as processing of single objective function, premature convergence, low efficiency of optimization, etc. To deal with multiobjective optimization problems, several extended GAs are presented based on the SGA. Muruta and Ishibuchi [26] developed a GA-based algorithm to solve multiobjective problems called multiobjective genetic algorithm (MOGA). Dynamic weighting is used in this algorithm to transfer the multiple objectives into a single objective. Deb et al. [27] proposed the nondominated sorting GA-II (NSGA-II) approach, which is implemented with an effective sorting method based on individual ranking by nondominated sorting and a crowded distance sorting evaluating the population density of solutions in the same rank [28]. Huo et al. [29] employed an SGA and a cooperative coevolutionary genetic algorithm (CCGA) to solve the disc cutters' multispiral and stochastic layout problems. Shahsavar et al. [30] compared three self-adaptive multiobjective evolutionary algorithms for a triple-objective project scheduling problem, including self-adaptive multipopulation genetic algorithm (SAMPGA), two-phase subpopulation genetic algorithm (TPSPGA), and nondominated ranked genetic algorithm (NRGA). Considering the characteristics of the above GAs and requirements in structure design of cutter rings, an SAMPGA [31] has been selected in this paper as an appropriate optimization algorithm.

In this paper, a multiobjective optimization design model of structural parameters for disc cutter rings, including five objectives and twelve constraints, is established based on the engineering technical requirements and the corresponding cutter ring structure design requirements. According to the characteristics of this model, an SAMPGA is applied to solve the multiobjective optimization design problem, and the fuzzy analytical hierarchy process (FAHP) is employed to deal with the multiobjective functions. Finally, the applicability and validity of the proposed approach are demonstrated through a case study in a TBM project.

2. Problem Description and Modeling

2.1. Requirements in Structure Design of Cutter Ring. A disc cutter ring is the only part of a disc cutter that contacts with rock, and its structure characteristics directly determine the cutter service performance. To obtain the disc cutter with high rock breaking efficiency and long service life, purpose,

and principle of the cutter ring structural design are summarized by consulting relevant literature and engineering data. (1) Excellent rock breaking performance: Disc cutter can break rock normally and break more rocks as much as possible under harsh geological conditions, which is the basic requirement of the cutter ring geological adaptability design. (2) Minimum cutter energy consumption for rock breaking: Breaking rocks efficiently with less energy consumption will improve the overall tunneling efficiency of disc cutter and cutterhead. (3) Long service life and uniform wear: Loads that cutter bearings suffered meet the design requirement, and the blade shape of cutter ring maintains stability during normal wear process. (4) Meet the basic structural parameters requirement of cutter ring: There is a correlation among the structural parameters of the CCS disc cutter ring; therefore, the setting of structural parameters should meet the relevant requirements. (5) Meet the requirements of cutterhead drive performance: Total loads on the disc cutter should not exceed the rated thrust and torque of the cutterhead. (6) Meet the ultimate load-bearing capability requirements of disc cutter: Average load of the disc cutter after optimization should not exceed the prescribed limit load.

2.2. Mathematical Model and Parameter Expression. Multiobjective optimization design model for cutter ring structural parameters mainly includes objective functions, constraints, and design variables, which can be defined as follows:

$$\begin{aligned} \min \quad & f_m(x_1, x_2, \ldots, x_n), \quad m = 1, 2, \ldots, M, \\ \text{s.t.} \quad & g_k(x_1, x_2, \cdots, x_n) \geq 0, \quad k = 1, 2, \ldots, K, \\ & h_l(x_1, x_2, \ldots, x_n) = 0, \quad l = 1, 2, \ldots, L, \\ & x_i^{\mathrm{L}} \leq x_i \leq x_i^{\mathrm{U}}, \quad i = 1, 2, \ldots, N, \end{aligned} \tag{1}$$

where $f_m(x)$ is the objective functions, X denotes the decision space, $x = (x_1, x_2, \ldots, x_n) \in X$, x^{L} and x^{U} are lower and upper boundaries of design variable x, respectively, $g_k(x)$ is the k-th inequality constraint, and $h_l(x)$ is the l-th equality constraint.

CCS disc cutter is the most commonly used type of cutter for TBM due to its balanced rock breaking and wear resistance performance. Thus, it is set as the structural design object in this paper. Sketch of disc cutter and cutter ring is shown in Figure 1. The key structural parameters of the cutter ring, including cutter tip width T, edge angle θ, and edge radius r, are selected as the design variables, which can be expressed as $x = (T, \theta, r)$.

2.3. Objective Functions

2.3.1. Rock Breaking Capability of Disc Cutter. Cutter rock breaking capability is the key factor to the smooth excavation for TBM in hard rock conditions, and it is a basic criterion reflecting the geological adaptability. Rock breaking induced by disc cutter is a process of crack generation, crack propagation, crack intersection, and rock fragmentation. Therefore, the length of the side crack induced by disc cutter is used to characterize the cutter rock breaking capability, which can be calculated by Liu's semiempirical and semitheoretical model [32]:

Before the formation of the crushed zone,

$$L = \left[\left(\frac{F_V}{\sigma_c d^2} + 0.10848\right) \times \frac{F_V}{38.49109}\right]^{2/3} \times \left(\frac{1 - \upsilon^2}{EG_{IC}}\right)^{1/3}. \tag{2}$$

After the formation of the crushed zone,

$$L = \left[\left(\frac{F_V}{\sigma_c d^2} - 2.45434\right) \times \frac{F_V}{27.86853}\right]^{2/3} \times \left(\frac{1 - \upsilon^2}{EG_{IC}}\right)^{1/3}, \tag{3}$$

where F_V is the normal force of disc cutter, σ_c is uniaxial compressive strength (UCS) of rock, d is the size of the cutter tip, $d = T/\cos(\theta/2) + 2r$, υ is Poisson's ratio of rock, E is Young's modulus of rock, and G_{IC} is the energy release rate of rock.

Forces of disc cutter can be obtained by using the Colorado School of Mines (CSMs) model [33] as follows:

$$\begin{aligned} F_V &= F_t \cos\left(\frac{\varphi}{2}\right) = C\frac{\varphi RT}{1 + \psi}\left(\frac{S\sigma_c^2\sigma_t}{\varphi\sqrt{RT}}\right)^{1/3} \cos\left(\frac{\varphi}{2}\right), \\ F_R &= F_t \sin\left(\frac{\varphi}{2}\right) = C\frac{\varphi RT}{1 + \psi}\left(\frac{S\sigma_c^2\sigma_t}{\varphi\sqrt{RT}}\right)^{1/3} \sin\left(\frac{\varphi}{2}\right), \\ \varphi &= \arccos\left(\frac{R - h}{R}\right), \end{aligned} \tag{4}$$

where F_t denotes the total force of disc cutter, F_R is the rolling force of disc cutter, R is the radius of disc cutter, ψ is the distribution coefficient of cutter tip pressure, φ denotes the contact angle between cutter ring and rock, h is the cutting depth, S is the cutter spacing, C is a dimensionless coefficient with value of 2.12, and σ_t is the tensile strength of rock. The rest of the symbols have the same meaning as equations (2) and (3). Additionally, the meanings of the same symbolic variables used in the following equations are consistent.

Based on the linear elastic fracture theory, the relationship of the energy release rate G_{IC} and the fracture toughness K_{IC} can be defined as [34]

$$G_{IC} = \frac{(1 - \upsilon^2)K_{IC}^2}{E}. \tag{5}$$

According to Zhang's research [35], the fracture toughness K_{IC} can be approximately computed by the following equation:

$$K_{IC} = 0.145\sigma_t. \tag{6}$$

Therefore, the objective function of cutter rock breaking capability is defined as

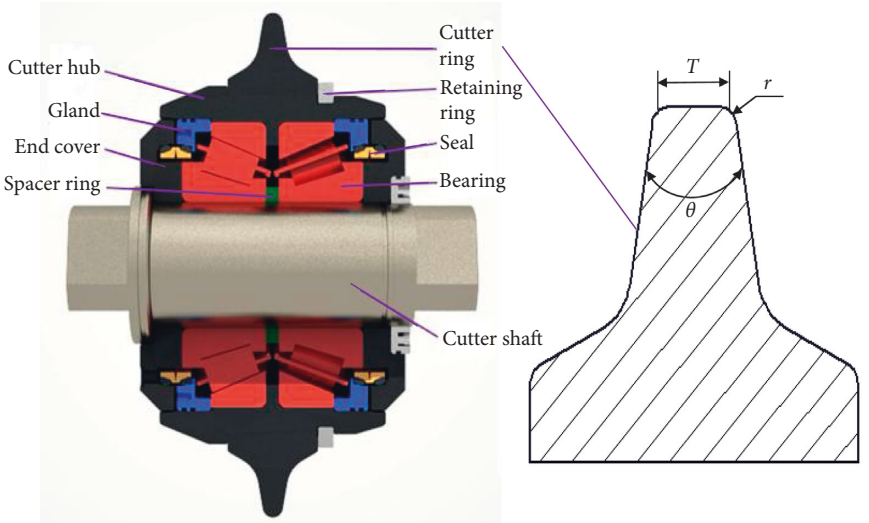

Figure 1: Sketch of disc cutter and cutter ring.

$$\min f_1(x) = \frac{1}{L}. \tag{7}$$

2.3.2. Energy Consumption for Rock Breaking by Disc Cutter. Specific energy (SE) of disc cutter refers to the energy consumed by breaking the unit volume of rock, and the greater the SE is, the lower the rock breaking efficiency is. The following equations can be used to calculate the value of SE [36, 37]:

For $L < h\tan(\beta/2)$,

$$E_S = \begin{cases} \dfrac{F_R}{\mu Sh}, & 0 < S \le 2L + T, \\ \dfrac{F_R}{\left[Sh - \left((S-T)^2/4\tan(\beta/2)\right)\right]}, & 2L + T < S \le 2h\tan\left(\dfrac{\beta}{2}\right) + T, \\ \dfrac{F_R}{\left(h^2\tan(\beta/2) + Th\right)}, & S > 2h\tan\left(\dfrac{\beta}{2}\right) + T. \end{cases} \tag{8}$$

For $L \ge h\tan(\beta/2)$,

$$E_S = \begin{cases} \dfrac{F_R}{\mu Sh}, & S \le 2L + T, \\ \dfrac{F_R}{\left(h^2\tan(\beta/2) + Th\right)}, & S > 2L + T, \end{cases} \tag{9}$$

where β is the rock breakage angle and μ is the coefficient characterizing the direction of side crack propagation.

Then, the objective function of cutter energy consumption for rock breaking is defined as

$$\min f_2(x) = E_S. \tag{10}$$

2.3.3. Load-Bearing Capability of Cutter Bearing. When the disc cutter breaks rock, the cutter bearings suffer large axial and radial loads and high-intensity impact vibration. Failure of the bearing is an important reason for the abnormal failure of the disc cutter. When calculating the bearing life, it is necessary to convert the bearing's radial and axial loads into equivalent loads. The equation for calculating the equivalent dynamic bearing load is as follows:

$$P = f_p\left(XF_n + YF_a\right), \tag{11}$$

where X and Y are the radial load factor and axial load factor for the bearing, respectively, F_n is actual radial bearing load, F_a is the actual axial bearing load, and f_p is the load coefficient related to working conditions.

The bearing with relatively large load is selected as the design object, and its actual radial and axial loads are calculated as follows:

$$\begin{cases} F_n = \dfrac{\sqrt{F_V^2 + F_R^2}}{2} + \dfrac{F_S D_z}{2L_z}, \\ F_a = \dfrac{F_n}{2y} + F_S, \end{cases} \tag{12}$$

where D_z is the outside diameter of bearing, L_z is the center distance between two bearings, $L_z = T_b + l$, T_b is the bearing width, l is the thickness of spacer ring, y is the derived axial force coefficient, F_S is the side force of disc cutter [38], $F_S = (\tau/2)\cdot(R\varphi)^2\cdot\sin(R\varphi/2\rho)$, τ is the shear strength of rock, and ρ is the installation radius of disc cutter.

The objective function for the load-bearing capability of cutter bearing is defined as

$$\min f_3(x) = P. \tag{13}$$

2.3.4. Wear Life of Cutter Ring. Wear life of the cutter ring is mainly characterized by wear loss, which is related to the cutter working conditions, the structural parameters of cutter ring, and the layout parameters of disc cutter. Based on Archard's abrasive wear theory, Zhu [39] established a

theoretical model of the front and side wear loss (wear step) for the cutter ring. The calculations are as follows:

Front wear step of the cutter ring:

$$dh_1 = k_D \times \int_0^{\varphi/\omega} \left[\left(C \sqrt[3]{\frac{S}{\varphi\sqrt{RT}} \cdot \sigma_c^2 \sigma_t} \left(1 - \frac{\varphi - \omega t}{\varphi} \right)^{\psi} \right) \times \sqrt{(\omega R(1 - \cos(\varphi - \omega t)) + v \sin(\varphi - \omega t))^2 + (\omega_1 R \sin(\varphi - \omega t))^2} \right]. \tag{14}$$

Side wear step of the cutter ring:

$$dh_2 = k_D \times \frac{c \cdot \cos(\xi) \cdot \cos(\theta/2) \cdot \cos(\gamma)}{\sin((\beta/2) - (\theta/2) - \xi - \gamma) \cdot \cos(\beta/2)} \times \int_0^{(\arccos((R-h)/r_c))/\omega} \left[fr_c \times \sqrt{\left(\omega \sqrt{r_c^2 + R^2 - 2Rr_c \cos(\varphi - \omega t)} \right)^2 + v^2 + 2v\omega r_c \sin(\varphi - \omega t)} \right] dt, \tag{15}$$

where ω is the rotating angular velocity of disc cutter, $\omega = \rho\omega_1/R$, ω_1 is the rotating angular velocity of cutterhead, $\omega_1 = \pi n/30$, n is the rotating speed of cutterhead, v is the tunneling speed of cutterhead, $v = hn/60$, t is the wear time, K_D is the wear coefficient, c is the rock cohesion, ζ is the internal friction angle of rock, γ is friction angle between rock and cutter, r_c is the distance from a point on the cutter edge side to the center axis of disc cutter, and fr_c is the lateral pressure distribution coefficient.

In the actual TBM project, when the front of a cutter ring is worn to the limit value, the cutter ring will be replaced immediately. Therefore, the wear life of the cutter ring can be expressed as

$$w_h = \frac{w_{\max} R}{60\, dh_1 \cdot n \cdot \rho}, \tag{16}$$

where $w_{\max}$ is the limit wear volume of the cutter ring.

The objective function for wear life of the cutter ring can be defined as

$$\min f_4(x) = \frac{1}{w_h}. \tag{17}$$

2.3.5. Wear Uniformity of Cutter Ring. Changing trend of the cutter blade is different when disc cutter works and wears in different geological conditions. Actually, the shape of the worn blade is determined by both front wear and side wear [39]. If the cutter blade shape (blade angle) is stable in the wear process, the advantage of CCS disc cutter can be exerted and the optimal wear resistance performance will be obtained.

According to the geometric relationship between the front-side wear steps and the cutter blade shape, the objective function of the wear uniformity of cutter ring is defined as

$$\min f_5(x) = \left(\frac{dh_2}{dh_1} - \tan\left(\frac{\theta}{2} \right) \right)^2. \tag{18}$$

From the above optimization objective functions, it can be found that the cutter ring structural design problem contains several mutually conflicting objectives. The optimization objectives of disc cutter cannot be satisfied simultaneously under the same structural parameters, which require compromise among multiple objectives. In this paper, weight coefficient transformation method [40] is used to deal with the multiobjective optimization problem, which transforms the multiobjective functions into a single objective function. By giving different weight coefficients to the objective functions according to specific geological conditions, the geological adaptability optimization result can be achieved for cutter ring structural design. By using the weight coefficient transformation method, the combined objective function can be expressed as follows:

$$\min f(x) = \sum_{i=1}^{5} \left(w_i \cdot \frac{f_i(x)}{\chi_i} \right), \tag{19}$$

where w_i is weight coefficient and χ_i is the elimination coefficient set for eliminating the order of magnitude difference [41].

2.4. Subject to Constraints

2.4.1. Dimensional Constraints of Geometric Structures. Cutter tip width is the main structural parameter of the cutter ring. A very small tip width will aggravate the cutter wear and increase the cost of cutter replacement, while a very large width will increase the rock breaking force and weaken the penetration capability of disc cutter. Considering the commonly used parameters, the dimensional constraint of the cutter tip width is given:

$$\begin{aligned} g_1(x) &= T - 0.012 \geq 0, \\ g_2(x) &= 0.03 - T \geq 0. \end{aligned} \tag{20}$$

Cutter edge angle has a great influence on the rock breaking performance of disc cutter. Choice of sharp-edged

and flat-edged cutters is the primary consideration in cutter structure design. Considering the changing trend of the blade shape in the wear process, the dimensional constraint for the cutter edge angle is defined as

$$\begin{aligned} g_3(x) &= \theta - 10^\circ \geq 0, \\ g_4(x) &= 30^\circ - \theta \geq 0. \end{aligned} \tag{21}$$

Too small cutter edge radius will result in stress concentration and difficulty in penetrating hard rocks. When the cutter edge radius is larger than 10 mm, the influence of edge radius parameter on cutting force will be reduced. Therefore, the dimensional constraint for the cutter edge radius is defined as

$$\begin{aligned} g_5(x) &= r - 0.0025 \geq 0, \\ g_6(x) &= 0.01 - r \geq 0. \end{aligned} \tag{22}$$

Spacer ring not only plays a role in positioning but also determines the starting torque of disc cutter. The dimensional constraint of spacer ring thickness is set as follows:

$$\begin{aligned} g_7(x) &= l - 0.01 \geq 0, \\ g_8(x) &= 0.018 - l \geq 0. \end{aligned} \tag{23}$$

2.4.2. Dimensional Correlation Constraint of Geometric Structures. In addition to satisfying the above dimensional constraints, the structural parameters of the cutter ring also need to satisfy the following correlation constraints:

$$g_9(x) = \frac{T}{2} - r \times \tan\left(\frac{\pi}{4} - \frac{\theta}{4}\right) > 0. \tag{24}$$

2.4.3. Constraint of Ultimate Load-Bearing Capability of Disc Cutter. The ultimate load-bearing capability of disc cutter varies with cutter ring size. Ultimate load-bearing capability of 17-inch disc cutter is 250 kN and that of 19-inch cutter is 315 kN [12]. Thus, the constraint of cutter ultimate load-bearing capability is given as

$$g_{10}(x) = F_V \leq F_{\text{rated}}. \tag{25}$$

2.4.4. Constraint of Cutterhead Drive Performance. The constraint of cutterhead drive performance is defined as

$$\begin{aligned} g_{11}(x) &= F_R \leq \frac{T_d}{0.3\,DN}, \\ g_{12}(x) &= F_V \leq \frac{2F_d}{D}, \end{aligned} \tag{26}$$

where F_d and T_d are the rated thrust and torque of cutterhead, respectively, and D is the diameter of cutterhead.

3. Description of Methodologies

Cutter ring structural design problem contains several mutually conflicting objectives as well as linear and nonlinear constraints, which belongs to a discontinuous multiobjective optimization problem. Therefore, an improved self-adaptive multipopulation genetic algorithm (SAMPGA) is used to solve this problem. Meanwhile, the fuzzy analytic hierarchy process (FAHP) is employed to deal with multiple objective functions and to obtain the combined objective function.

3.1. Self-Adaptive Multipopulation Genetic Algorithm. As is stated above, GA is one of the widely used evolutionary algorithms to deal with nonlinear optimization problems. However, after the broad application of GA, many shortcomings of SGA have been exposed constantly, for instance, the processing of single objective function, premature convergence, low efficiency of optimization. To overcome the defects of SGA, an improved self-adaptive multipopulation genetic algorithm (SAMPGA) is introduced to solve the multiobjective optimization design model for cutter ring structural parameters. The steps of SAMPGA are described as follows, where a general scheme is depicted in Figure 2.

(1) Constructing objective functions: The multiple objective functions and combined objective function are demonstrated in Section 2.3.

(2) Initialization: Assuming the number of populations is M, the number of individuals in each subpopulation is N. Crossover and mutation are the core operators of GA. According to the characteristics of SAMPGA, each population is given different crossover and mutation probabilities to balance the global and local search capability. The crossover probability P_c and mutation probability P_m are initialized as follows:

$$\begin{aligned} P_c &= 0.7 + (0.9 - 0.7) \times \text{rand}(M, 1), \\ P_m &= 0.01 + (0.1 - 0.01) \times \text{rand}(M, 1). \end{aligned} \tag{27}$$

(3) Constructing fitness function: To prevent local convergence or divergence owing to the over-small fitness value, the fitness function is constructed according to equation (20) as follows:

$$\text{Fitness} = \frac{2}{1 + \sum_{i=1}^{5} \omega_i \left(f_i(x)/\chi_i\right)}. \tag{28}$$

(4) Selection: A roulette-based nonlinear ranking selection strategy is adopted in this approach.

(5) Crossover: SGA is not sufficiently flexible to generate offspring by means of a single crossover of different chromosomes. In this paper, the crossover operator is set up by combining the multipoint crossover and uniform crossover.

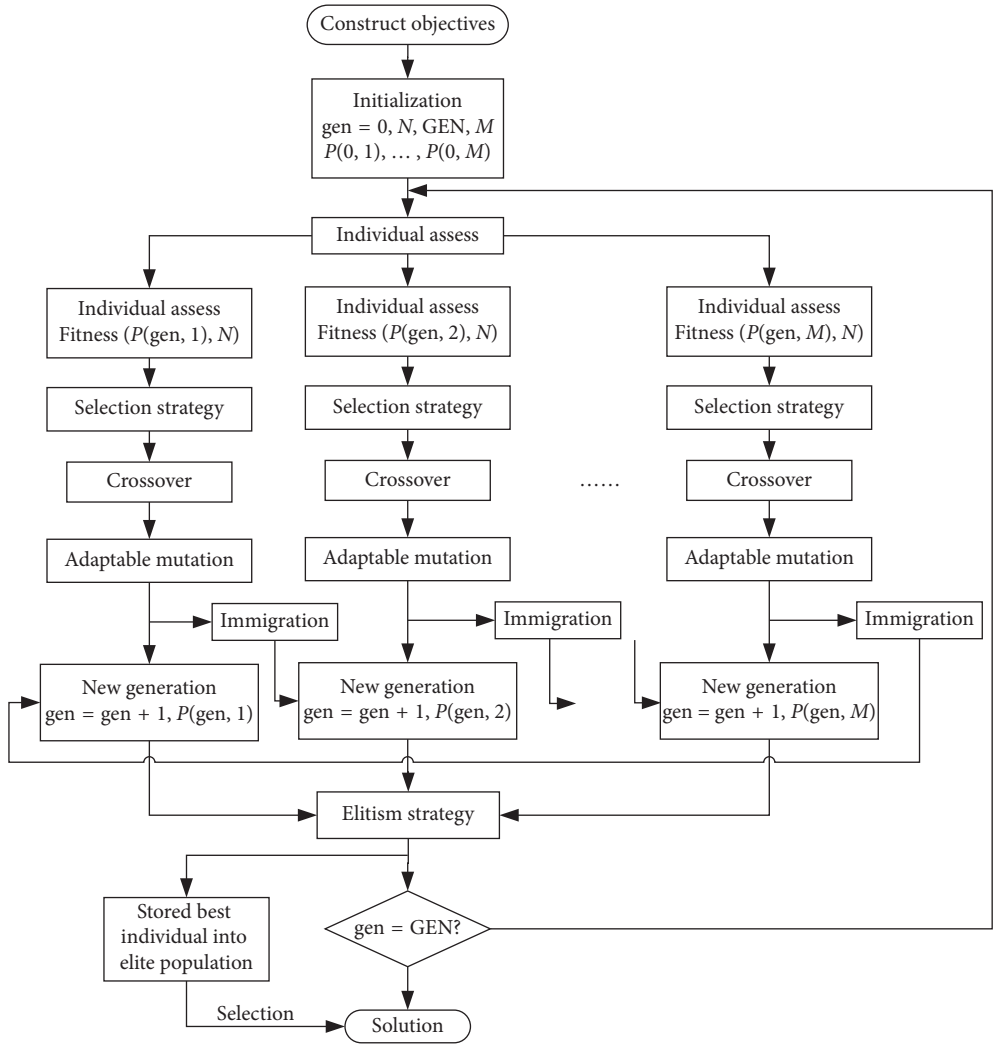

Figure 2: Framework of SAMPGA.

(6) Self-adaptable mutation: Mutation is the main factor affecting the convergence and optimal result of GA in the later stage. Mutation of SGA is usually constant and is independent of the number of iterations. In order to improve the global search capability in the early stage, the crossover of SGA is usually set to 0.7–0.9 and the mutation is set to 0.001–0.05, which may lead to premature local convergence and is not conducive to obtaining the optimal result in the later stage. To overcome the aforementioned problem, the self-adaptable mutation operator is adopted in this study. The mutation probability is self-adjusted after each generation of operation and increases gradually with the increase in the number of iterations. The dynamic changing equation is shown as follows:

$$P_m(i+1) = P_m(i) + \left(\frac{\text{gen}}{\text{GEN}}\right)^m \times \left(\frac{P_c}{\varsigma} - P_m(i)\right), \quad (29)$$

where gen is the number of iteration, GEN is the total number of iterations, m is the calculation precision digit of mutation operator, and ς is the changing coefficient, value of which is set to 7–9 according to the crossover probability.

(7) Immigrant and elitism strategy: At the end of each iteration, immigrant operator is applied to screen out the best and worst individuals of the current population and then substitute the best individual for the worst individual in the population, thus realizing multipopulation coevolution. Through the elitism strategy, the best individuals in each population are recorded and stored into the elite population. The elite population is updated in each iteration. Finally, the optimal individual is found out across all subpopulations.

3.2. Fuzzy Analytical Hierarchy Process. When solving the multiobjective optimization design problem of disc cutter ring, the different assignment of weight coefficients for multiple objective functions will exhibit a significant influence on the design result of cutter ring structure. Meanwhile, setting different weight coefficients for

objectives based on the geological conditions is the core of the cutter ring geological adaptability design. To obtain a suitable coefficient set, the fuzzy analytic hierarchy process (FAHP) is introduced on the basis of the expert investigation. The process of calculating the weight coefficients for cutter ring objective functions by decision makers using the fuzzy AHP can be displayed as follows [42].

Let $O = \{o_1, o_2, \ldots, o_n\}$ be an object set and $G = \{g_1, g_2, \ldots, g_m\}$ be a goal set. $M_{gi}^1, M_{gi}^2, \ldots, M_{gi}^m$ ($i = 1, 2, \ldots, n$) are the extent analysis values for each object, where M_{gi}^j ($j = 1, 2, \ldots, m$) are triangular fuzzy numbers (TFNs) provided in Table 1.

(1) The value of fuzzy synthetic extent with respect to i-th object is defined as

$$S_i = \sum_{j=1}^{m} M_{gi}^j \otimes \left[\sum_{i=1}^{n}\sum_{j=1}^{m} M_{gi}^j\right]^{-1}, \tag{30}$$

where

$$\sum_{j=1}^{m} M_{gi}^j = \left(\sum_{j=1}^{m} l_i^j, \sum_{j=1}^{m} m_i^j, \sum_{j=1}^{m} u_i^j\right),$$
$$\left[\sum_{i=1}^{n}\sum_{j=1}^{m} M_{gi}^j\right]^{-1} = \left(\frac{1}{\sum_{i=1}^{n}\sum_{j=1}^{m} u_i^j}, \frac{1}{\sum_{i=1}^{n}\sum_{j=1}^{m} m_i^j}, \frac{1}{\sum_{i=1}^{n}\sum_{j=1}^{m} l_i^j}\right). \tag{31}$$

(2) The degree of possibility of $M_2 = (l_2, m_2, u_2) \geq M_1 = (l_1, m_1, u_1)$ is defined as

$$V(M_2 \geq M_1) = \operatorname{hgt}(M_1 \cap M_2) = \mu_{M_2}(\mathrm{po}) = \begin{cases} 1, & m_2 \geq m_1, \\ 0, & l_1 \geq u_2, \\ \dfrac{l_1 - u_2}{(m_2 - u_2) - (m_1 - l_1)}, & \text{otherwise}, \end{cases} \tag{32}$$

where μ (po) is the largest intersection between two TFNs.

(3) The degree of possibility for convex fuzzy numbers to be greater than k convex fuzzy numbers M_i is defined as

$$V(M \geq M_1, M_2, \ldots, M_k) = V[(M \geq M_1), (M \geq M_2), \ldots, (M \geq M_k)] = \min V(M \geq M_i), \quad i = 1, 2, \ldots, k. \tag{33}$$

Assuming that $d'(A_i) = \min V(S_i \geq S_k)$, $k = 1, 2, \ldots, n$ ($k \neq i$), the weight coefficient vector can be determined as

$$W' = \left(d'(A_1), d'(A_2), \ldots, d'(A_n)\right)^T, \tag{34}$$

where A_i ($i = 1, 2, \ldots, n$) are n elements.

(4) The final weight coefficient vector is determined as

$$W = \left(d(A_1), d(A_2), \ldots, d(A_n)\right)^T = \left(w_1, w_2, \ldots, w_n\right)^T, \tag{35}$$

where nonfuzzy number W is the normalization of W'.

Based on SAMPGA and FAHP, a new multiobjective optimization method is proposed for the cutter ring structural design, the flow chart of which is depicted in Figure 3.

4. Case Study

4.1. Background. The multiobjective optimization design method is applied to optimize the structural parameters of the cutter ring used in a water conveyance project, located in northeast China. Total length of the TBM construction section in this project is 19.8 km, the main formation across this section is II-III type granite and II-III-IV tuff. The tunnel is excavated using a TBM with a diameter of 8 m, and four double-edged 17-inch (432 mm) center disc cutters and forty-three 19-inch (483 mm) front and edge disc cutters are installed on the TBM cutterhead. A 19-inch front disc cutter is selected as a design object, and two typical construction sections (section A and section B) are selected as the geologic background. The main rock type in section A is granite, and the UCS of the rock reaches to 90–140 MPa. In section B, the main rock type is tuff, and the UCS of the sampled rock is approximately 40–90 MPa. Cutter spacing of this disc cutter is 83 mm, and radius of the cutter ring is 241.3 mm. Cutting depth is 6 mm and average rotational speed of cutterhead is 6.67 r/min in section A, while the average penetration of cutter is 10 mm and average rotational speed of cutterhead is 6.67 r/min in section B. The bearing used for this cutter is Timken H926749/10.

4.2. Comparison of Optimization Results between SAMPGA and GA. To verify the convergence and robustness of the improved SAMPGA, an experiment is performed, in which the rock breaking capability of disc cutter is set as the objective function and section A is chosen as the geological condition. The results are compared with those of SGA. For the two GAs, the evolutionary generation is set to 1000 and the total number of individuals is 500. SGA parameters are set to be 0.8 for crossover probability, 0.05 for mutation

Table 1: Linguistic variables and triangular fuzzy numbers.

Linguistic scale	Fuzzy number	Triangular fuzzy number	Triangular fuzzy reciprocal
Equal importance (EI)	$\tilde{1}$	(1, 1, 1)	(1, 1, 1)
Equal to moderate importance (IMI)	$\tilde{2}$	(1, 2, 3)	(1/3, 1/2, 1)
Moderate importance (MI)	$\tilde{3}$	(2, 3, 4)	(1/4, 1/3, 1/2)
Moderate to strong importance (ISI)	$\tilde{4}$	(3, 4, 5)	(1/5, 1/4, 1/3)
Strong importance (SI)	$\tilde{5}$	(4, 5, 6)	(1/6, 1/5, 1/4)
Strong to very strong importance (IVSI)	$\tilde{6}$	(5, 6, 7)	(1/7, 1/6, 1/5)
Very strong importance (VSI)	$\tilde{7}$	(6, 7, 8)	(1/8, 1/7, 1/6)
Very strong to extreme importance (IEXI)	$\tilde{8}$	(7, 8, 9)	(1/9, 1/8, 1/7)
Extreme importance (EXI)	$\tilde{9}$	(8, 9, 10)	(1/10, 1/9, 1/8)

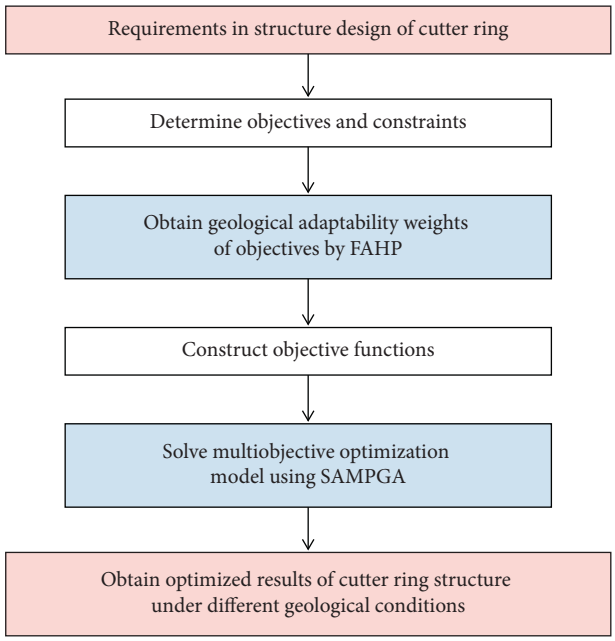

Figure 3: Flow chart of cutter ring structural design based on the proposed method.

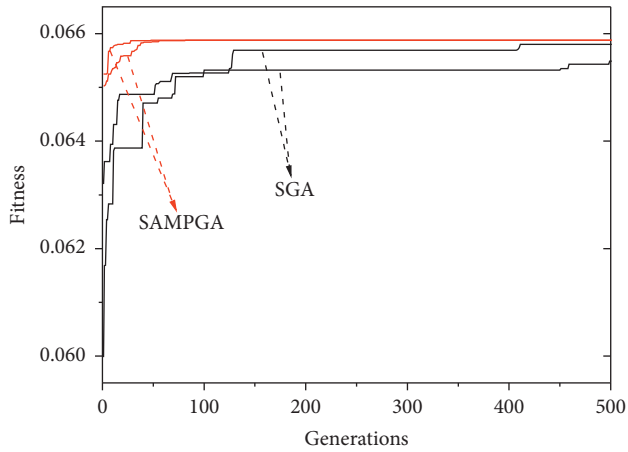

Figure 4: Fitness curves of SGA and SAMPGA.

probability [43], along with roulette strategy. SAMPGA parameters are set to 10 for populations and 50 for individuals per population. Initializations of crossover and mutation probabilities vary in different subpopulations. Specifically, the crossover probability is set to be 0.7–0.9 and mutation probability is set 0.01–0.1 [30, 44], and the mutation probability dynamically increases with the increase of computational generation. The optimization results obtained by SGA and SAMPGA are listed in Tables 2 and 3, where C.G. denotes convergence generation and C.T. denotes convergence time. Figure 3 shows the comparison of fitness curves for SGA and SAMPGA. From Tables 2 and 3 and Figure 3, the following conclusions can be drawn:

(1) The results of the five operations of SGA are quite different. The minimum value of the optimized objective function is 15.2059 and the maximum value is 15.2742, which indicates the poor stability and premature local convergence in SGA. The results of five experiments of SAMPGA are identical, and the optimal value is 15.1782, indicating SAMPGA performs better than SGA in terms of the three structural parameters in all the tests.

(2) Figure 3 shows that the two fitness curves obtained by SGA are quite different, and there are still mutations in the later stage of operation. As a contrast, the fitness curves obtained by SAMPGA has little difference and is stable to the same value in the later period, indicating SAMPGA exhibits a better performance in stability and convergence than SGA.

(3) The average convergence generation of SGA is beyond 400, whereas SAMPGA converges to the optimal results before 150 generations. From Tables 2 and 3, the computation time of SGA is less than that of SAMPGA. However, since the convergence generation of SAMPGA is far less than that of SGA, a smaller evolutionary generation can be set up for SAMPGA to weaken the disadvantage of computing time compared with SGA in practical application.

4.3. Multiobjective Optimization Results of Structural Parameters for Cutter Rings. To solve the multiobjective optimization model, weight coefficients of each objective function need to be determined using FAHP firstly. With the example of computing the weight coefficients of objective functions under the granite condition, the processes of weights determination are demonstrated. Eight experienced decision makers from TBM manufacturer, cutter manufacturer, construction company, and related academic institution are invited to fill in questionnaires using the

Table 2: Results obtained by SGA.

Number	T (mm)	θ (°)	r (mm)	f_1 (m^{-1})	C.G.	C.T. (s)
1	29.8584	29.7827	9.9687	15.2416	616	9.896
2	29.9205	29.9676	9.9998	15.2059	411	9.726
3	29.9944	28.4154	9.9658	15.2141	595	9.527
4	29.8737	29.3454	9.9903	15.234	383	10.079
5	29.8866	25.6863	9.994	15.2742	409	9.839

Table 3: Results obtained by SAMPGA.

Number	T (mm)	θ (°)	r (mm)	f_1 (m^{-1})	C.G.	C.T. (s)
1	30	30	10	15.1782	161	19.399
2	30	30	10	15.1782	104	19.303
3	30	30	10	15.1782	94	19.435
4	30	30	10	15.1782	141	19.503
5	30	30	10	15.1782	123	19.372

linguistic variables in Table 1, so as to establish the fuzzy aggregated decision matrix. For a group decision environment with k experts, fuzzy aggregated decision matrix can be obtained using equation (36). Table 4 exhibits the final fuzzy aggregate decision matrix of objectives under the granite condition, where O_1, O_2, O_3, O_4, and O_5 denote the objectives of rock breaking capability, energy consumption for rock breaking, load-bearing capability, wear life, and wear uniformity, respectively.

$$\begin{cases} \widetilde{x}_{ij} = \left(Lx_{ij}, Mx_{ij}, Ux_{ij}\right), \\ Lx_{ij} = \min\limits_{k}\left\{Lx_{ijk}\right\}, \\ Mx_{ij} = \dfrac{1}{K}\sum\limits_{k=1}^{K} Mx_{ijk}, \\ Ux_{ij} = \max\limits_{k}\left\{Ux_{ijk}\right\}, \end{cases} \tag{36}$$

where $\widetilde{x}_{ij}$ is the arithmetic mean of TFNs constructed by k experts.

The fuzzy synthetic extents of the objectives are presented as follows by using equation (30):

$$\begin{aligned} S_1 &= (6, 13, 25) \otimes (0.0136, 0.0273, 0.0601) \\ &= (0.0816, 0.3553, 1.5036), \\ S_2 &= (1.61, 2.905, 4.5) \otimes (0.0136, 0.0273, 0.0601) \\ &= (0.0218, 0.0793, 1.2706), \\ S_3 &= (3.583, 8.472, 17) \otimes (0.0136, 0.0273, 0.0601) \\ &= (0.0487, 0.2315, 1.0224), \\ S_4 &= (2.7, 5.847, 11) \otimes (0.0136, 0.0273, 0.0601) \\ &= (0.0367, 0.1598, 0.6616), \\ S_5 &= (2.733, 6.361, 16) \otimes (0.0136, 0.0273, 0.0601) \\ &= (0.0371, 0.1738, 0.9623). \end{aligned} \tag{37}$$

Computations of the degree of possibility (V value) are depicted in Table 5 by using equation (32).

Using equation (33), the minimum values of degree of possibility are obtained. By using equations (34) and (35), the final normalized weight coefficients under granite geological condition in section A are obtained as: $W_1 = (0.2585, 0.1052, 0.2286, 0.1933, 0.2144)^T$. By using the above-mentioned method, the final weight coefficient set under tuff condition is obtained as $W_2 = (0.2511, 0.1403, 0.1332, 0.2874, 0.188)^T$. Ranking orders of weight coefficients for the five objectives under granite geological condition are $O_1 > O_3 > O_5 > O_4 > O_2$, while those of coefficients under tuff condition become $O_4 > O_1 > O_5 > O_2 > O_3$. By analyzing the weight coefficients under different geological conditions, it is indicated TBM experts and project builder pay more attention to the objectives of rock breaking capability, load-bearing capability, and wear life under the harsh geological conditions with high rock strength (i.e., granite condition), whereas the wear resistance performances (O4 and O5) become the topmost objectives and load-bearing capability changes to the low-level one in tuff geological condition. Since the rock is more difficult to break under hard rock conditions (in section A), the bearing life is significantly affected by the strong impact and heavy load during rock breaking and the wear of the cutter ring is more serious due to the high strength rock. Therefore, O1, O3, and O5 are selected as the extreme importance objectives in the experts' opinions. However, loads of the cutter ring are relatively small when it breaks rock with low strength (in section B), and the main failure form of the cutter is normal wear; thus, the wear resistance performance objectives (O4 and O5) along with rock breaking capability are the most important objectives under tuff condition.

Fitness function is constructed by equation (19) and the weight coefficient of each objective function. SAMPGA is applied to solve the multiobjective optimization model, and the optimized results are obtained and listed in Table 6. Structural parameters of the original disc cutter used in this TBM project are 19.05 mm in cutter tip width, 20° in edge angle, and 5 mm in edge radius.

From Table 6, it can be seen that the values of optimized cutter tip width and edge angle have been reduced while the value of edge radius is slightly increased compared with those of the original cutter ring under the granite condition. After optimization, the optimization objectives are improved except for the wear life of the cutter ring. The values of the objective functions of rock breaking capability, energy consumption, load-bearing capability, and wear uniformity decrease by 13.7%, 5.7%, 12.9%, and 22.1% respectively, while that of wear life increase by 2.6%. Because there are several mutually conflicting objectives in the model and the coupling relationship between objective functions and variables is complex, the improvement of one optimization objective is often accompanied by the degradation of another objective. Thus, it is usually impossible to obtain an optimal individual adapting to all objectives in the optimization process. Due to the relatively low weight of wear life, it is deteriorated in the optimization process, which improves the comprehensive performance of cutter ring.

Table 4: Fuzzy aggregated decision matrix.

	O_1	O_2	O_3	O_4	O_5
O_1	(1, 1, 1)	(2, 5.167, 10)	(1, 2, 4)	(1, 2.333, 5)	(1, 2.5, 5)
O_2	(0.1, 0.227, 0.5)	(1, 1, 1)	(0.167, 0.464, 1)	(0.2, 0.486, 1)	(0.143, 0.728, 1)
O_3	(0.25, 0.556, 1)	(1, 2.833, 6)	(1, 1, 1)	(1, 1.833, 4)	(0.333, 2.25, 5)
O_4	(0.2, 0.514, 1)	(1, 2.5, 5)	(0.25, 0.639, 1)	(1, 1, 1)	(0.25, 1.194, 3)
O_5	(0.2, 0.542, 1)	(1, 2.5, 7)	(0.2, 0.736, 3)	(0.333, 1.583, 4)	(1, 1, 1)

Table 5: Calculations of degree of possibility (V value).

	S_1	S_2	S_3	S_4	S_5
$V(S_1 \geq \ldots)$	—	1	1	1	1
$V(S_2 \geq \ldots)$	0.4065	—	0.5931	0.7441	0.7119
$V(S_3 \geq \ldots)$	0.8838	1	—	1	1
$V(S_4 \geq \ldots)$	0.7478	1	0.8951	—	0.978
$V(S_5 \geq \ldots)$	0.8291	1	0.9405	1	—

Table 6: Optimization results of structural parameters for the cutter ring.

Geological conditions	Design objective	T (mm)	θ (°)	r (mm)	f_1 (m^{-1})	f_2 ($MJ \cdot m^3$)	f_3 (kN)	f_4 ($\times 10^{-3} h^{-1}$)	f_5
Granite	Original cutter ring	19.05	20	5	31.29	79.18	153.25	4.23	6.92
	Optimized cutter ring	16.1	10.61	7.4	26.99	74.61	133.41	4.34	5.39
	Variation (%)				−13.7	−5.7	−12.9	2.6	−22.1
Tuff	Original cutter ring	19.05	20	5	27.38	34.54	98.17	1.81	5.33
	Optimized cutter ring	21.02	15.49	5.77	19.69	35.51	101.4	1.64	4.81
	Variation (%)				−28.1	2.8	3.3	−9.4	−9.8

Under tuff geological condition, the values of optimized cutter tip width and edge radius increase slightly while that of edge angle decreased compared with those of the original cutter. The values of the objective functions of rock breaking capability, wear life, and wear uniformity decrease by 28.1%, 9.4%, and 9.8%, respectively, while those of energy consumption and load-bearing capability increase by 2.8% and 3.3%.

Comparing the optimized results of cutter ring structural parameters under different geological conditions, the cutter tip width under granite condition is smaller than that of original cutter and is contrary under tuff condition. Besides, the cutter edge angle under granite condition is smaller than that of in tuff condition, indicating that it is appropriate to apply the cutter ring with narrow edge and small blade angle in high strength rock condition. When cutting the low-strength rock such as tuff, the cutter tip width should be increased appropriately considering the wear resistance performance. The optimization results of cutter ring structural parameters vary with different geological conditions, which indicate that the geological adaptability should be considered in the design of cutter ring. The proposed design method in this paper determines the weight coefficients of objective functions based on expert knowledge and FAHP under different geological conditions, which realizes the geological adaptability design for cutter ring structure. Additionally, it is revealed in Table 6 that the performance improvement of disc cutter under granite is more significant than that under tuff after optimization and the structural parameters of cutter ring change little under tuff condition compared with the original cutter ring, demonstrating that the original disc cutter is more suitable for the rock with low strength. The above finding has been verified by practical applications of disc cutters. In the actual construction process, original disc cutters exhibit excellent rock breaking performance and long service life under the tuff geological condition. Daily tunneling progress of TBM can reach to 30 m, and the wear rate of the cutter ring is approximate 0.08–0.12 mm/m. In addition, disc cutters suffer little abnormal failure, and the wear of cutter ring is uniform, which verifies that the original disc cutter is suitable for tuff geology.

5. Conclusions

In this paper, a multiobjective optimization design method for structural parameters of cutter ring is developed by combining an SAMPGA and FAHP, and the conclusions are drawn as follows:

(1) Based on the complex geological conditions and the corresponding cutter ring structure design requirements, a multiobjective optimization model is established to design the structural parameters of disc cutter ring. The rock breaking capability, energy consumption, load-bearing capability, wear life, and wear uniformity of disc cutter are selected as the objectives, and the geometric structure of cutter ring, ultimate load-bearing capability, and cutterhead drive performance are determined as constraints. An SAMPGA is utilized to deal with the optimization problem, and FAHP is employed to combine the multiple objectives into a single objective function.

(2) The proposed method is applied to a case study of cutter ring structure design in a TBM project. After

optimization, the rock breaking performance and service life of the disc cutter are improved. For granite condition, the performances of rock breaking capability, energy consumption, load-bearing capability, and wear uniformity are improved by 13.7%, 5.7%, 12.9%, and 22.1% respectively, and the performance of wear life is deteriorated by 2.6%. The performances of rock breaking capability, wear life, and wear uniformity are improved by 28.1%, 9.4%, and 9.8%, respectively, while those of energy consumption and load-bearing capability are deteriorated by 2.8% and 3.3% under tuff geological condition.

(3) The optimized results obtained by SAMPGA are better than those of SGA in the tests. The convergence generation of SAMPGA is smaller than that of SGA, and the robustness of SAMPGA is better than that of SGA. The utilization of SAMPGA effectively solves the premature and local convergence problems during structural optimization.

(4) Geological adaptability should be considered in the design of cutter ring. Rock breaking capability, load-bearing capability, and wear uniformity should be considered as the topmost objectives when cutting high-strength rock, while wear life and rock breaking capability should be given priority under low-strength rock condition. It is appropriate to apply the cutter ring with a narrow edge and small blade angle in granite condition, whereas the cutter tip width should be increased appropriately considering the wear resistance performance in tuff condition. The geological adaptability design for cutter ring structure is realized by using the proposed method based on the dynamic weight coefficients.

It should be noted the objective functions of the optimization design model are solved on the premise that the cutter ring can invade the rock smoothly, which is satisfied in the aforementioned TBM project. However, in some TBM project, the UCS of the surrounding rock that TBM encountered will reach to 200 MPa or even more than 300 MPa. It is difficult for disc cutter to penetrate and break rock under such harsh geological conditions. At this time, the TBM builders prefer to replace the conventional cutter ring with heavy narrow-edged cutter ring. Therefore, the penetration capability, as well as stiffness-strength of the disc cutter, should be considered and added to the model in the future work. Moreover, other relevant objectives (e.g., the number of rock cracks) will be taken into account to improve the proposed method.

Data Availability

The data used to support the findings of this study are included within the article.

Conflicts of Interest

The authors declare no conflicts of interest.

Acknowledgments

This work was supported by the National Key R&D Program of China (no. 2018YFB1306700), the National Natural Science Foundation of China (no. 51905550), the Project funded by China Postdoctoral Science Foundation (no. 2019M652795), the National Basic Research Program of China (no. 2013CB035401), and the Project of Key Technology and Integrated Demonstration for Green Remanufacturing of Shield Machines.

References

[1] N. Afrasiabi, R. Rafiee, and M. Noroozi, "Investigating the effect of discontinuity geometrical parameters on the TBM performance in hard rock," *Tunnelling and Underground Space Technology*, vol. 84, pp. 326–333, 2019.

[2] J. Huo, H. Wu, W. Sun, Z. Zhang, L. Wang, and J. Dong, "Electromechanical coupling dynamics of TBM main drive system," *Nonlinear Dynamics*, vol. 90, no. 4, pp. 2687–2710, 2017.

[3] L. Lin, Y. Xia, Q. Mao, and X. Zhang, "Experimental study on wear behaviors of TBM disc cutter ring in hard rock conditions," *Tribology Transactions*, vol. 61, no. 5, pp. 920–929, 2018.

[4] J. Liu, W. Wan, Y. Chen, and J. Wang, "Dynamic indentation characteristics for various spacings and indentation depths: a study based on laboratory and numerical tests," *Advances in Civil Engineering*, vol. 2018, Article ID 8412165, 12 pages, 2018.

[5] J. Rostami, "Study of pressure distribution within the crushed zone in the contact area between rock and disc cutters," *International Journal of Rock Mechanics and Mining Sciences*, vol. 57, pp. 172–186, 2013.

[6] C. Balci and D. Tumac, "Investigation into the effects of different rocks on rock cuttability by a V-type disc cutter," *Tunnelling and Underground Space Technology*, vol. 30, pp. 183–193, 2012.

[7] D. Tumac and C. Balci, "Investigations into the cutting characteristics of CCS type disc cutters and the comparison between experimental, theoretical and empirical force estimations," *Tunnelling and Underground Space Technology*, vol. 45, pp. 84–98, 2015.

[8] S. W. Choi, S. H. Chang, Y. T. Park, G. P. Lee, and G. J. Bae, "Experimental evaluation of the effects of cutting ring shape on cutter acting forces in a hard rock," *Journal of Korean Tunnelling and Underground Space Association*, vol. 15, no. 3, pp. 225–235, 2013.

[9] B. Chiaia, "Fracture mechanisms induced in a brittle material by a hard cutting indenter," *International Journal of Solids and Structures*, vol. 38, no. 44-45, pp. 7747–7768, 2001.

[10] A. Lislerud, *Principles of Mechanical Excavation (No. POS-IVA--97-12)*, Posiva Oy, Eurajoki, Finland, 1997.

[11] X.-P. Zhang, P.-Q. Ji, Q.-S. Liu, Q. Liu, Q. Zhang, and Z.-H. Peng, "Physical and numerical studies of rock fragmentation subject to wedge cutter indentation in the mixed ground," *Tunnelling and Underground Space Technology*, vol. 71, pp. 354–365, 2018.

[12] J. Roby, T. Sandell, J. Kocab, and L. Lindbergh, "The current state of disc cutter design and development directions," in *Proceeding of the 2008 North American Tunneling Conference, SME C*, vol. 4, pp. 36–45, San Francisco, CA, USA, 2008.

[13] B. Maidl, L. Schmid, W. Ritz, and M. Herrenknecht, *Hardrock Tunnel Boring Machines*, John Wiley & Sons, Hoboken, NJ, USA, 2008.

[14] M. F. Marji, "Simulation of crack coalescence mechanism underneath single and double disc cutters by higher order displacement discontinuity method," *Journal of Central South University*, vol. 22, no. 3, pp. 1045–1054, 2015.

[15] W. Sun, L. Guo, J. J. Zhou, and J. Z. Huo, "Rock fragmentation simulation under dual TBM disc cutter and design of cutter ring," *Journal of China Coal Society*, vol. 40, no. 6, pp. 1297–1302, 2015.

[16] J. Li, Y. F. Nie, K. Fu, C. Ma, J. B. Guo, and M. X. Xu, "Experiment and analysis of the rock breaking characteristics of disc cutter ring with small edge angle in high abrasive grounds," *Journal of the Brazilian Society of Mechanical Sciences and Engineering*, vol. 40, no. 10, p. 505, 2018.

[17] Y. M. Xia, T. Ouyang, L. Chen, D. Z. Luo, and X. M. Zhang, "Study on the influencing factors of the disc cutter performance," *Journal of Basic Science and Engineering*, vol. 20, no. 3, pp. 500–507, 2012.

[18] J.-H. Yang, X.-P. Zhang, P.-Q. Ji et al., "Analysis of disc cutter damage and consumption of TBM1 section on water conveyance tunnel at Lanzhou water source construction engineering," *Tunnelling and Underground Space Technology*, vol. 85, pp. 67–75, 2019.

[19] R. V. Rao, D. P. Rai, and J. Balic, "Multi-objective optimization of abrasive waterjet machining process using Jaya algorithm and PROMETHEE Method," *Journal of Intelligent Manufacturing*, vol. 30, no. 5, pp. 2101–2127, 2019.

[20] M. Kilinc and J. M. Caicedo, "Finding plausible optimal solutions in engineering problems using an adaptive genetic algorithm," *Advances in Civil Engineering*, vol. 2019, Article ID 7475156, 9 pages, 2019.

[21] M. Aghbashlo, M. Tabatabaei, M. H. Nadian, V. Davoodnia, and S. Soltanian, "Prognostication of lignocellulosic biomass pyrolysis behavior using ANFIS model tuned by PSO algorithm," *Fuel*, vol. 253, pp. 189–198, 2019.

[22] M. Duma and B. Twala, "Sparseness reduction in collaborative filtering using a nearest neighbour artificial immune system with genetic algorithms," *Expert Systems with Applications*, vol. 132, pp. 110–125, 2019.

[23] N. D. Hoang, Q. L. Nguyen, and Q. N. Pham, "Optimizing construction project labor utilization using differential evolution: a comparative study of mutation strategies," *Advances in Civil Engineering*, vol. 2015, Article ID 108780, 8 pages, 2015.

[24] Y. Li, H. Soleimani, and M. Zohal, "An improved ant colony optimization algorithm for the multi-depot green vehicle routing problem with multiple objectives," *Journal of Cleaner Production*, vol. 227, pp. 1161–1172, 2019.

[25] A. A. Zaidan, B. Atiya, M. R. Abu Bakar, and B. B. Zaidan, "A new hybrid algorithm of simulated annealing and simplex downhill for solving multiple-objective aggregate production planning on fuzzy environment," *Neural Computing and Applications*, vol. 31, no. 6, pp. 1823–1834, 2019.

[26] T. Muruta and H. Ishibuchi, "MOGA: multi-objective genetic algorithm," in *Proceedings of 1995 IEEE International Conference on Evolutionary Computation*, Perth, WA, Australia, November-December 1995.

[27] K. Deb, A. Pratap, S. Agarwal, and T. Meyarivan, "A fast and elitist multiobjective genetic algorithm: NSGA-II," *IEEE Transactions on Evolutionary Computation*, vol. 6, no. 2, pp. 182–197, 2002.

[28] H. A. Leyva, E. Bojórquez, J. Bojórquez et al., "Earthquake design of reinforced concrete buildings using NSGA-II," *Advances in Civil Engineering*, vol. 2018, Article ID 5906279, 11 pages, 2018.

[29] J. Huo, W. Sun, J. Chen, and X. Zhang, "Disc cutters plane layout design of the full-face rock tunnel boring machine (TBM) based on different layout patterns," *Computers & Industrial Engineering*, vol. 61, no. 4, pp. 1209–1225, 2011.

[30] A. Shahsavar, A. A. Najafi, and S. T. A. Niaki, "Three self-adaptive multi-objective evolutionary algorithms for a triple-objective project scheduling problem," *Computers & Industrial Engineering*, vol. 87, pp. 4–15, 2015.

[31] M. Zandieh and N. Karimi, "An adaptive multi-population genetic algorithm to solve the multi-objective group scheduling problem in hybrid flexible flowshop with sequence-dependent setup times," *Journal of Intelligent Manufacturing*, vol. 22, no. 6, pp. 979–989, 2011.

[32] H. Y. Liu, *Numerical modelling of the rock fragmentation progressive process by mechanical tools*, Ph.D. thesis, Lulea University of Technology, Luleå, Sweden, 2004.

[33] J. Rostami, "Hard rock TBM cutterhead modeling for design and performance prediction," *Geomechanik und Tunnelbau*, vol. 1, no. 1, pp. 18–28, 2008.

[34] B. N. Whittaker, R. N. Singh, and G. Sun, *Rock Fracture Mechanics: Principles, Design, and Applications*, Vol. 570, Elsevier, Amsterdam, Netherlands, 1992.

[35] Z. X. Zhang, "An empirical relation between mode I fracture toughness and the tensile strength of rock," *International Journal of Rock Mechanics and Mining Sciences*, vol. 39, no. 3, pp. 401–406, 2002.

[36] Y. M. Xia, B. Guo, G. Q. Cong, X. H. Zhang, and G. Y. Zeng, "Numerical simulation of rock fragmentation induced by a single TBM disc cutter close to a side free surface," *International Journal of Rock Mechanics and Mining Sciences*, vol. 91, pp. 40–48, 2017.

[37] Q. Tan, N. E. Yi, Y. M. Xia, Y. Zhu, X. H. Zhang, and L. K. Lin, "Study of calculation equation of TBM disc cutter optimal spacing," *Rock and Soil Mechanics*, vol. 37, no. 3, pp. 883–892, 2016.

[38] Z. H. Zhang and D. H. Ye, "The model of the disc cutter's broken-rock and the calculation of its side-force," *Journal of Basic Science and Engineering*, vol. 12, no. 3, pp. 293–298, 2004.

[39] Z. H. Zhu, "Numerical simulation of disc cutter's wear evolution for tbm," Central South University, Changsha, China, Master Thesis, 2013.

[40] Y. Zhang, M. Harman, and S. A. Mansouri, "The multi-objective next release problem," in *Proceedings of the 9th Annual Conference on Genetic and Evolutionary Computation*, pp. 1129–1137, ACM, London, UK, July 2007.

[41] W. Luo, Y. H. Chen, and G. H. Zhang, "Optimization of parameters for planar internal gear primary-enveloping crown worm drive," *Journal of Mechanical Engineering*, vol. 50, no. 7, pp. 1–7, 2014.

[42] P. Sirisawat and T. Kiatcharoenpol, "Fuzzy AHP-TOPSIS approaches to prioritizing solutions for reverse logistics barriers," *Computers & Industrial Engineering*, vol. 117, pp. 303–318, 2018.

[43] J.-S. Kim, C.-G. Kim, and C.-S. Hong, "Optimum design of composite structures with ply drop using genetic algorithm and expert system shell," *Composite Structures*, vol. 46, no. 2, pp. 171–187, 1999.

[44] L. Wang, J.-C. Cai, and M. Li, "An adaptive multi-population genetic algorithm for job-shop scheduling problem," *Advances in Manufacturing*, vol. 4, no. 2, pp. 142–149, 2016.